THE JOURNAL OF PHYSICAL CHEMISTRY C
A JOURNAL OF THE AMERICAN CHEMICAL SOCIETY

pubs.acs.org/JPCC

Article

Photochemical Fluorination of TiO_2(110) Produces an Atomically Thin Passivating Layer

William J. I. DeBenedetti and Melissa A. Hines*

Cite This: *J. Phys. Chem. C* 2022, 126, 4899−4906

Read Online

ACCESS | Metrics & More | Article Recommendations | Supporting Information

ABSTRACT: Fluorine has been widely reported to improve the photoreactivity of TiO_2 nanocrystals, but surface science studies of this enhancement have been stymied by the lack of well controlled fluorination chemistries. Fluorine-terminated rutile (110) surfaces were produced by the photochemical degradation of solution-prepared trimethyl acetate monolayers in the presence of XeF_2 (g) at room temperature. X-ray photoemission spectroscopy showed that the fluorinated surfaces were terminated by 0.8 monolayers of F bound to initially undersaturated Ti atoms. The fluorinated surface remained notably contamination free, even after immersion in solution and exposure to air for tens of minutes. The contamination-resistant properties of the fluorinated surface were attributed to the random blocking of 80% of the undersaturated Ti atoms, which simulations showed would block 93% of bidentate binding sites. This fluorine termination was very robust. Immersing the fluorinated surface in boiling H_2O for 60 min or boiling base for 10 min removed only ∼60% of the F atoms. Although the initial TiO_2(110) surface was atomically flat, scanning tunneling microscopy images showed that the fluorinated surface was rough on an atomic scale, displaying short, atomically straight rows parallel to the [001] direction. The roughened morphology was indication of a relatively isotropic etching reaction. This isotropy was attributed to both the destabilization of the surface by F as well as the unusual reaction dynamics of XeF_2. The increased reactivity of the fluorinated surface toward etching can be rationalized in terms of disrupted charge balance in the surface layer. Consistent with this, density functional theory simulations showed that the removal of bridging O atoms from the fully fluorinated surface to produce O_2 would be exoergic.

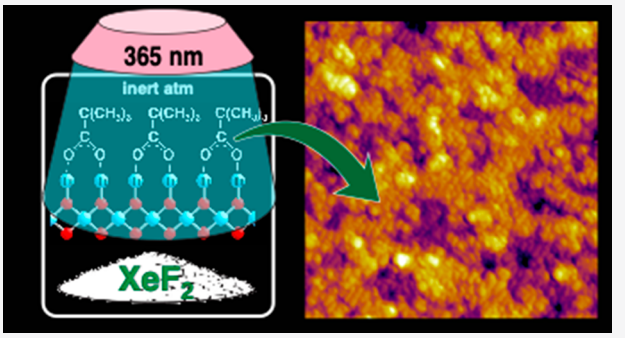

INTRODUCTION

The passivation of semiconductor surfaces to unwanted reactions is important to many fields, from the fabrication of silicon transistors[1] to the generation of efficient perovskite solar cells[2] to the production of quantum-dot-based photovoltaics.[3] These passivating layers are typically relatively thick on an atomic scale. As a result, they usually obscure the underlying structure of the substrate and often act as a barrier to charge transfer. In contrast, atomically thin passivating layers are relatively rare, with the most notable being hydrogen-terminated silicon.[4,5]

Our interest in F-terminated TiO_2 was piqued by a recent observation that fluorinated anatase TiO_2 nanocrystals, which contain both surface and subsurface F atoms, remain clean (i.e., carbon free) even after immersion in solution and exposure to air for tens of minutes.[6] This behavior, while surprising, is consistent with *ab initio* calculations that predicted that F-terminated anatase would have an exceptionally low surface energy.[7] Based on this this observation, we hypothesized that F atoms might passivate TiO_2 by binding to the undersaturated Ti atoms, forming a repellent coating.

Fluorinated nanocrystals behave very differently than "clean," adsorbate-free TiO_2 surfaces, which spontaneously develop a monolayer-thick coating of adsorbed formic and acetic acids when they are exposed to air.[8] The adsorbed acids are the result of ppb-level concentrations of organic acids in air, which are formed by the degradation of volatile biogenic hydrocarbons such as isoprene. The formation of this robust monolayer is due to the strong, bidentate bonds between the adsorbed acids and undersaturated surface Ti atoms. The acid monolayers cannot be desorbed cleanly, at least in vacuum, as the temperatures needed for desorption lead to partial decomposition of the acids.[9]

Our interest in the effects of F on TiO_2 was also stimulated by the observation that F is a shape-control agent—and thus a reactivity-control agent—in TiO_2 nanocrystal growth. The addition of F to TiO_2 growth solutions leads to the production of anatase TiO_2 single crystals with a variety of shapes and

Received: January 26, 2022
Revised: February 21, 2022
Published: March 4, 2022

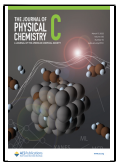

https://doi.org/10.1021/acs.jpcc.2c00651
J. Phys. Chem. C 2022, 126, 4899−4906

reactivities.[7,10] Many studies have also shown that F doping or surface fluorination of TiO_2 enhances the photocatalytic degradation of organic molecules in aqueous solutions, including benzoic acid,[11] benzene,[12] phenols,[13] and organic dye molecules.[14,15] Fluorine also enhances photocatalytic H_2 (g) production on Pt/TiO_2 via the water splitting reaction.[16,17] A number of researchers have postulated that F doping shifts the local charge balance in TiO_2,[18] stabilizing near-surface oxygen vacancies and Ti^{3+},[10,17] which are known to affect surface reactivity.[19−21]

To further understand the properties of fluorinated TiO_2, we have developed a new synthesis of F-terminated rutile TiO_2(110), the structure of which is sketched in Figure 1.

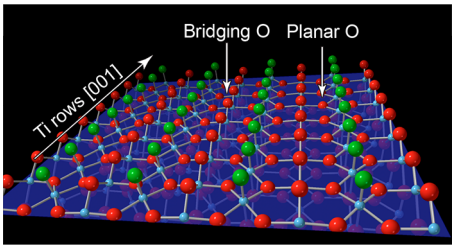

Figure 1. Structure of ideal F-terminated TiO_2(110) surface with 1.0 ML of F. The Ti, O, and F atoms are represented by blue, red, and green spheres, respectively.

Our synthesis uses XeF_2 as the fluorination agent, which is safer and easier to handle than F_2(g). The fluorination reaction etches the initially atomically flat TiO_2 surface, leaving a somewhat roughened morphology that is terminated by 0.8 monolayers (ML) of F bound to surface Ti atoms. (Here, we define 1 ML to be a surface density equivalent to one molecule per undersaturated Ti atom on a flat TiO_2(110) surface.)

As hypothesized, fluorine passivated the TiO_2 surface. The fluorinated surface was stable in air and resisted the adsorption of acids and other adventitious carbon species. The fluorination was also relatively stable in solution. Immersing the fluorinated surface in boiling H_2O for 60 min or boiling base for 10 min removed only ∼60% of the fluorination.

DFT simulations showed that adsorption of F to the undersaturated Ti atoms disrupted charge balance in the surface layer, partially oxidizing surface O atoms and significantly weakening their bonding. As a result, the removal of bridging O atoms from the fluorinated surface to form O_2 is predicted to be exoergic. We explained the etching of the surface in terms of both this disrupted charge balance and the unusual dynamics of XeF_2 reactivity.

METHODS

Experimental Methods. All solution-phase preparations were performed with glass or Teflon labware that had been cleaned as described previously.[22] Ultrapure H_2O (Millipore) was used throughout.

Atomically flat rutile TiO_2(110), which we refer to as "clean" TiO_2, was prepared by etching commercial samples (MTI Corp.) for 10 min in 1:1:2 28% NH_4OH:30% H_2O_2:H_2O by volume at 80 °C and rinsing in H_2O. The samples were optionally etched in 1:2 HCl:H_2O at 80 °C for 10 min to remove trace Sn, as sodium stannate is sometimes used as a H_2O_2 stabilizer.[23] Trimethylacetic acid (TCI America, >99%) was purified by sublimation in air. Trimethyl acetate (TMA) monolayers were prepared by immersing etched TiO_2 crystals for 10 min in a 200 mM aqueous or methanolic trimethylacetic acid solution at 65 °C. These monolayers are sensitive to photolytic degradation (*vide infra*), so this synthesis and subsequent handling were performed in the absence of fluorescent or UV radiation. The crystals were hydrophobic upon emersion and not rinsed after monolayer preparation. The crystal was transferred to a quartz reaction vessel that contained 75 mg of XeF_2 (s, Sigma-Aldrich, 99.99%), placed on a Schlenk line, flushed with inert gas, and sealed to produce ∼4 Torr of XeF_2 (g). The sample was irradiated with 6 mW/cm^2 of above-bandgap (365 nm) radiation from a UV diode array (Tektite) for 15 min to degrade the TMA monolayer into isobutene (g) and CO_2 (g). To ensure complete reaction, the sample was rinsed in H_2O, a second TMA monolayer was deposited, the surface was re-exposed to XeF_2 (g), and the sample was rinsed thoroughly in H_2O.

After preparation, the sample was transferred in air to an ultrahigh vacuum (UHV) analysis chamber equipped with a load lock. Scanning tunneling microscopy (STM) analysis was performed at room temperature with a W tip and typical tunneling conditions of 50−100 pA and 1.6−1.8 V. X-ray photoelectron spectroscopy (XPS) was performed using unmonochromated Mg Kα irradiation. Photoelectrons were collected at 70° from the surface normal to maximize surface sensitivity. A Tougaard baseline was removed from all reported spectra. The C 1s, F 1s, and Ti $2p_{3/2}$ spectra were normalized to the maximum amplitude of the Ti $2p_{3/2}$ transition, whereas the O 1s spectra were normalized to the maximum amplitude of the O 1s transition. Small energy corrections (∼0.1 eV) were applied to the reported spectra using reference energies to offset mild band bending. The same energy correction was applied to all spectra from a given sample.

Computational Methods. Density functional theory (DFT) was used to model the structure and energetics of fluorinated rutile (110) surfaces using 2 × 1 periodically repeating slabs consisting of five TiO_2 trilayers with autocompensated surfaces separated by a 12.5 Å vacuum spacing. Representative structures are shown in the Supporting Information. During optimization, the positions of the bottommost TiO_2 layer and its terminating bridging O rows were held fixed. Spin-polarized calculations were performed using DFT within the generalized gradient approximation[24] (GGA) using the revPBE functional[25] as implemented in the Vienna *ab initio* simulation package (VASP).[26−29] Hubbard on-site Coulomb interactions were included for the Ti d electrons with U = 4.1.[30−33] Long-range dispersion interactions were included using the DFT-D3(BJ) method with Becke-Johnson damping.[34,35] Electron−ion interactions were described using the projector augmented wave (PAW) method.[36,37] Electronic states were expanded in plane waves with a kinetic energy cutoff of 400 eV and a 6 × 6 × 1 Monkhorst−Pack grid of k points. Brillouin-zone integration was performed using Gaussian smearing.

RESULTS

HF Does Not Fluorinate TiO_2 at Room Temperature. There are many reports of TiO_2 surface fluorination by F^-- or HF-containing solutions;[38] however, in our hands, these procedures do not covalently bind F to TiO_2. For example, after a clean TiO_2 surface was immersed in 48% HF (aq) for 10 min at room temperature, XPS analysis showed that this treatment deposited 0.23 ML of fluorine-containing species on the surface; however, these species rinsed off with water,

https://doi.org/10.1021/acs.jpcc.2c00651
J. Phys. Chem. C 2022, 126, 4899−4906

leaving only a trace of fluorinated products (Supporting Information). The rinsed surface displayed the characteristic transitions of an organic acid monolayer (*vide infra*), which spontaneously develops on air-exposed TiO_2 surfaces.[8] Similar results were observed after immersion in 40% NH_4F (aq). Our conclusion was that these treatments produced F^- in the surface double layer (Helmholz layer), not covalently bound fluorine. Previous researchers have shown that the surface double layer is largely maintained upon substrate emersion,[39,40] but is removed by rinsing.

Researchers have fluorinated rutile (110) and TiO_2 nanocrystals by exposure to flowing anhydrous HF at elevated temperatures (200−500 °C) for hours.[41,42] We did not attempt this reaction due to the safety hazards associated with the procedure.

XeF_2 Does Not Fluorinate Air-Exposed TiO_2. XeF_2 (s) is a potent fluorinating agent that can be handled in air; the material sublimes easily and has a 4.5 Torr vapor pressure at 25 °C.[43]

When previously air-exposed clean TiO_2(110) surfaces were exposed to XeF_2 (g) at room temperature with or without above bandgap irradiation, no reaction was observed. Instead, photoemission spectra, represented by the blue curves in Figure 2, showed that the surface remained terminated by approximately a monolayer of organic acid bound to the undersaturated Ti sites on the surface.[8] The carboxylate moiety produced absorption features at 289.3 eV in the C 1s spectrum in Figure 2b and a shoulder at 532.5 eV in the O 1s spectrum in Figure 2c. A feature at 285.5 eV in the C 1s spectrum was assigned to a mixture of aliphatic C in the adsorbed acids and adventitious C. The F 1s transition in Figure 2a was barely detectable. The scale bars in the C 1s and F 1s spectra represent the intensity of 0.5 carboxylate C and 0.8 F atoms per unsaturated Ti atom, as discussed in the Supporting Information.

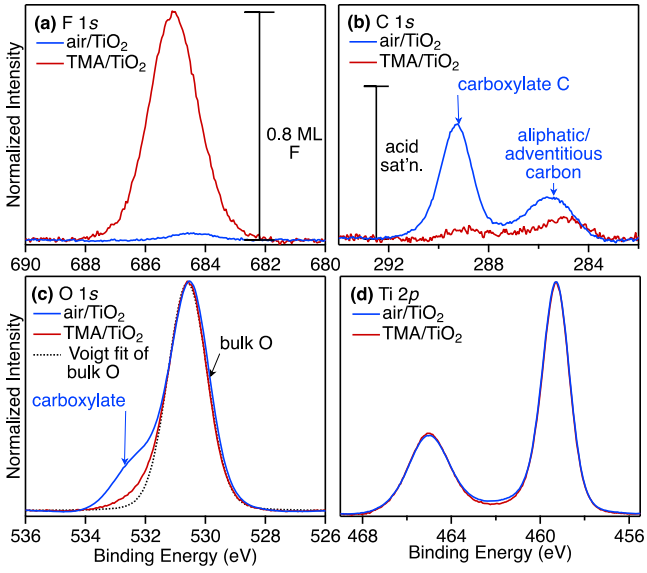

Figure 2. High resolution XP spectra of (blue) clean, air-exposed TiO_2 (unrinsed) and (red) trimethyl acetate-terminated TiO_2 after exposure to XeF_2 (g) and above bandgap radiation with subsequent H_2O rinsing. The panels show the (a) F 1s, (b) C 1s, (c) O 1s, and (d) Ti 2p regions. No reaction was observed on the air-exposed TiO_2 surface, whereas the initially TMA-terminated surface became fluorinated. The Voigt fit in panel c shows the slight asymmetry in the O 1s spectrum toward higher binding energy. The scale bars in the F 1s and C 1s spectra represent the intensity of 0.8 F atoms and 0.5 carboxylate C atoms per unsaturated Ti atom, respectively.

This experiment showed that XeF_2 does not fluorinate bridging O sites or other O sites when the undersaturated Ti sites are blocked.

Fluorination Requires Vacant Undersaturated Ti Sites. We hypothesized that XeF_2 was unable to fluorinate air-exposed TiO_2 surfaces because the most likely reactive sites, the undersaturated Ti atoms, were blocked by organic acids deposited from the air. To test this hypothesis, we devised a strategy to produce adsorbate-free TiO_2 surfaces *in situ*.

Previous researchers[44−46] have shown that trimethyl acetate (TMA) monolayers on TiO_2 can be photodecomposed in vacuum to generate purely gaseous products. This behavior appears to be unique to adsorbed tertiary acids, as photoexcitation produces a relatively stable tertiary radical. Other common carboxylate monolayers are stable to irradiation in vacuum.[47]

Figure 3a shows an STM image of a TMA-terminated TiO_2(110) surface prepared from methanolic solution. In this image, the TMA molecules are imaged as circular protrusions with a 2 × 1 periodicity that is due to the bidentate bonding of the acid to surface Ti atoms. Interestingly, these monolayers do not display the long-range ordering noted in some other carboxylate monolayers,[48] which we tentatively attribute to the steric bulk of TMA. Irradiation of this surface with above bandgap radiation in vacuum leads to the complete desorption of the monolayer and production of an adsorbate-free surface, as shown in Figure 3b. This reaction is induced by photoexcited holes generated in the TiO_2 crystal that diffuse to the surface and produce an excited oxidized carboxylate, which then decomposes to CO_2 (g) and isobutene (g).[46]

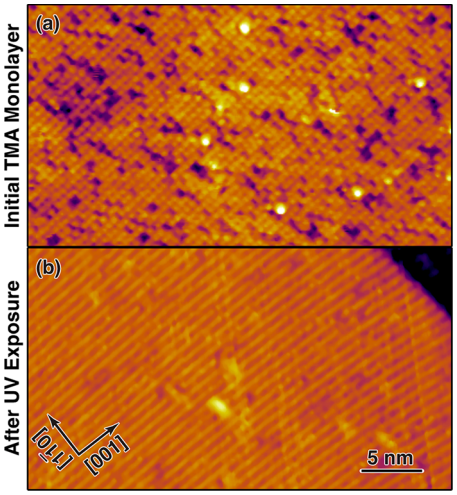

Figure 3. (a) STM image of trimethyl acetate-terminated TiO_2(110) surface prepared from methanolic solution. The dark spots are missing molecules that may have photodecomposed. The ∼10 white dots are unknown contaminants. (b) STM image of the same surface after illumination with 365 nm light in UHV, showing complete decomposition of the monolayer. The images are on the same scale.

To test our hypothesis, we exposed TMA-terminated TiO_2(110) to XeF_2 (g) at room temperature in the presence of above bandgap radiation. To ensure complete reaction, we then re-terminated the surface with TMA and re-exposed the surface to XeF_2. After reaction, the sample was thoroughly

https://doi.org/10.1021/acs.jpcc.2c00651
J. Phys. Chem. C 2022, 126, 4899−4906

rinsed in H_2O, producing a TiO_2 crystal with a partially fluorinated (0.8 ML) surface, as seen by the red XP spectra in Figure 2.

Undersaturated Ti Sites Are Fluorinated. The F 1s transition at 685.0 eV was assigned to F bound to an undersaturated Ti atom using calibrated DFT simulations. As described in the Supporting Information, DFT simulations of F 1s binding energies were calibrated against experimental data from small, fluorine-containing molecules.[49] The predicted binding energies of F bound to different sites on the TiO_2(110) surface are tabulated in Table 1.

Table 1. F 1s Binding Energies Observed in Experiment and Predicted by DFT Simulations

F binding site	bonding	B.E. (eV)
experimental		685.0
unsaturated Ti site	μ_1	684.3
bridging O site	μ_2	685.7
planar O site	μ_3	686.7
subsurface O site	μ_3	686.1

The μ_3-fluoro sites (i.e., planar or subsurface) were ruled out by their high binding energies. The replacement of a bridging O by F to form a μ_2-fluoro site was ruled out by the absence of a carboxylate transition in the O 1s spectrum. If F were to have replaced the bridging O sites, the undersaturated Ti sites would have been vacant, enabling adsorption of organic acids from the air, which was not observed.

The fluorinated surface was remarkably free of adventitious carbon or adsorbed acids as shown by the C 1s spectrum in Figure 2. The carboxylate C 1s transition was barely detectable, and we estimated the adsorbed acids to be ≤5% of the saturation coverage of 0.5 ML. This low density of carboxylate is consistent with 80% of the undersaturated Ti sites being blocked by F. As shown by the Monte Carlo simulation in Figure 4, if 80% of the undersaturated Ti sites were randomly

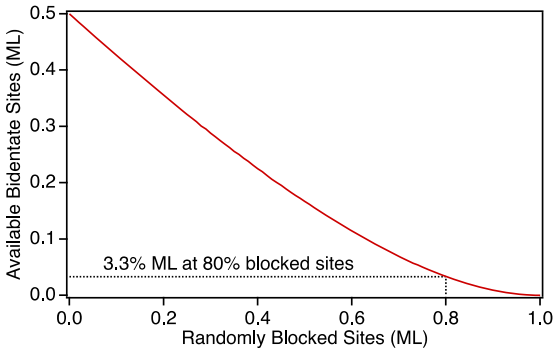

Figure 4. Simulated availability of bidentate undersaturated Ti binding sites on TiO_2(110) as a function of randomly adsorbed monodentate species (blocked sites). This Monte Carlo simulation predicted the adsorption of ~0.03 ML of organic acid in the presence of 0.8 ML of F bound to undersaturated Ti sites.

blocked, the surface could only adsorb 0.033 ML of bidentate molecules. This prediction is in good agreement with the ≤0.03 ML observed. The density of adventitious C was 2.5 atoms/nm^2, which is equivalent to 6% of a monolayer of graphene.

Fluorination Reaction Etches TiO_2. The fluorination reaction etches the initially atomically flat TiO_2 surface, leaving a somewhat roughened morphology. The initial preparation of clean TiO_2 surfaces in a hot, basic peroxide solution produces an atomically flat morphology with near-atomically straight step edges,[50] as seen in Figure 5a. After fluorination, the

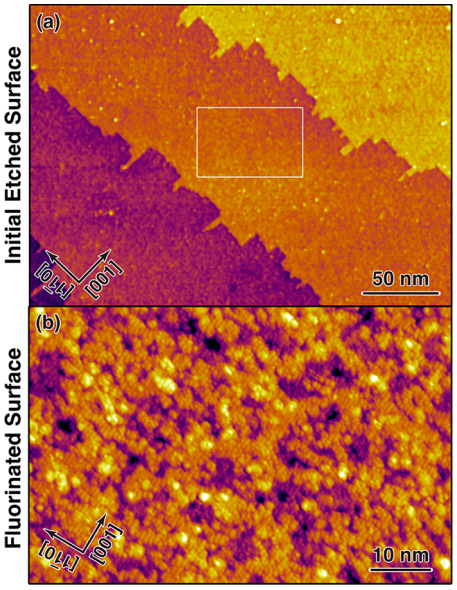

Figure 5. STM images of (a) initial atomically flat TiO_2(110) surface with vicinal steps produced by etching in a hot, basic peroxide solution and (b) surface after fluorination in XeF_2 and rinsing in H_2O, displaying very short atomic rows running along the [001] direction. The roughness of the fluorinated surface precluded the imaging of vicinal steps. The images are on very different scales, and the white rectangle in panel a indicates the relative area of panel b.

surface, shown in Figure 5b, was significantly rougher, displaying short straight rows parallel to the [001] direction, which we attributed to F-terminated Ti rows. In addition, single- and multi-layer etch pits are visible. There was no evidence of the (2 × 1) symmetry characteristic of organic acid absorption.

At this time, we do not know whether the etching happened during the reaction with XeF_2, during the H_2O rinse, or during both; however, we know that boiling H_2O further etched the fluorinated substrate. After a fluorinated crystal was immersed in boiling H_2O for 60 min, XPS analysis (Supporting Information) showed that 65% of the initial fluorine was removed. In addition, the F 1s transition shifted by 0.3 eV toward higher binding energy. This shift is consistent with DFT simulations, which predicted an 0.3 eV shift toward higher binding energy when one-half of the adsorbed F atoms were removed from a fully fluorinated surface.

In addition to these chemical changes, immersion in boiling H_2O significantly smoothed the fluorinated surface, as shown by the STM images in Figure 6. This treatment removed small islands on the surface and produced larger flat regions with visible atomic rows parallel to the [001] direction. The remaining islands had a weak crystallographic habit, suggesting anisotropic etching. Taken together, these chemical and morphological changes suggest that the fluorinated surface can be slowly etched by H_2O.

As a final test of the chemical stability of the fluorinated surface, we immersed a fluorinated sample in a boiling solution of 1:1 28% NH_4OH:H_2O by volume for 10 min. XPS analysis

https://doi.org/10.1021/acs.jpcc.2c00651
J. Phys. Chem. C 2022, 126, 4899−4906

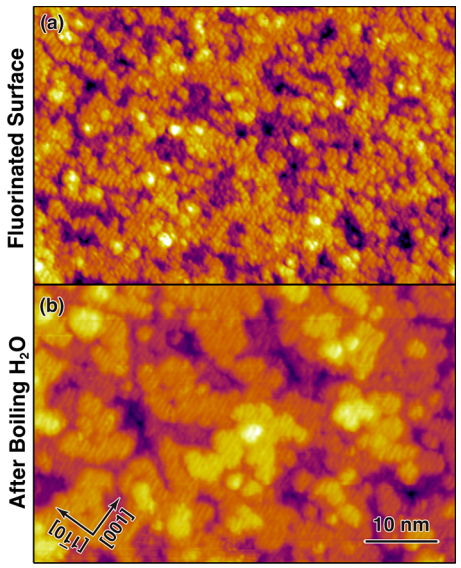

Figure 6. STM of fluorinated $TiO_2(110)$ surfaces before and after immersion in boiling H_2O for 15 min. Atomic rows running along the [001] direction are visible in both images. The boiling H_2O appears to etch the surface, as evidenced by the removal of small islands and the production of larger flat regions. The images are on the same scale.

(Supporting Information) showed that this treatment removed only 60% of the adsorbed fluorine.

In addition to its notable chemical stability, the fluorine monolayer resisted desorption at moderate temperatures, as shown by the data in Figure 7. In this experiment, a fluorinated sample was heated in UHV successively to 250 °C, 550 °C, and 650 °C, held at temperature for 20 min, then cooled to room temperature for XPS analysis. The only significant reaction was F desorption. At the highest temperature, the

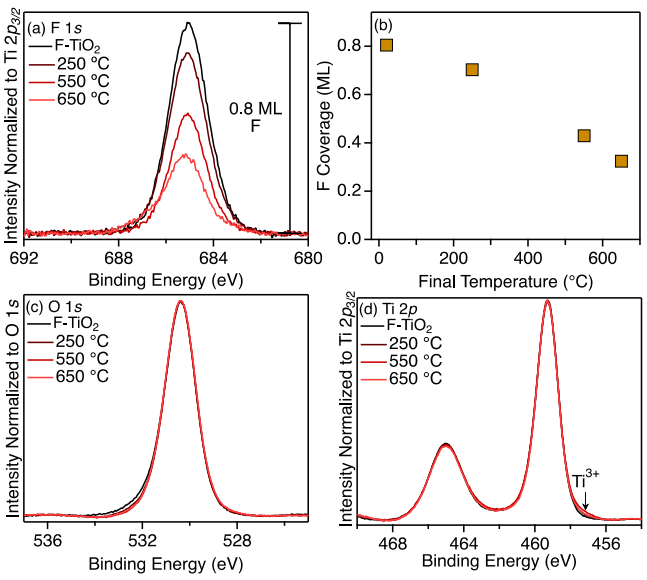

Figure 7. XPS analysis of fluorinated $TiO_2(110)$ as a function of successive 20 min heat treatments in UHV. High resolution spectra of the (a) F 1s, (c) O 1s, and (d) Ti 2p transitions and (b) the F surface coverage measured from the spectra in panel a. The scale bar on the F 1s spectra represents the intensity of 0.8 F atoms per unsaturated Ti atom.

TiO_2 was slightly reduced as indicated by the appearance of a small Ti^{3+} shoulder in the Ti 2p spectrum. Although some fluorine desorption was noted at 250 °C, one-third of the fluorine remained after heating at the highest temperature.

Fluorination Disrupts Formal Charge Balance, Increasing Reactivity. Rutile is a relatively inert material that is only etched slowly in very aggressive solutions, such as a hot basic peroxide solution,[51] so we were initially surprised by the significant etching seen in the STM images in Figure 5b. DFT simulations suggested that this behavior can be rationalized in terms of formal charge balance, which is also known as autocompensation.

The structure of the clean $TiO_2(110)$ surface with its alternating rows of bridging O atoms and undersaturated Ti atoms can be rationalized in terms of formal charge balance.[52] Each (110) plane contains twice as many O anions as Ti cations. In a purely ionic picture, each plane has a nominal formal charge of 0. In contrast, if the bridging O atoms on the surface were to be removed, the surface plane would be unbalanced and have a nominal positive charge. Electronic structure calculations have shown that the stability of structures that leave the surface neutral in a charge balance formalism can be attributed to the anion-derived surface states being completely filled and the higher-energy, cation-derived surface states being completely empty.[53]

The adsorption of F to the undersaturated Ti atoms disrupts charge balance in the surface layer. In a purely ionic view, the adsorbed F becomes F^- by oxidizing the bridging O^{2-} atoms to O^-. This behavior is manifested in two ways in DFT simulations of the fully fluorinated crystal. First and most importantly, the adsorption of a monolayer of F significantly destabilized the bridging O atoms, as shown by the calculated binding energies in Table 2. The bridging O atoms are strongly

Table 2. Calculated Binding Energies of Bridging O Atoms on Clean, Formate-Terminated, and Fluorine-Terminated $TiO_2(110)$

system	bridging O binding energy (eV)
clean	6.83
formate-TiO_2	7.08
F-TiO_2	2.40

bound to the clean surface, with Ti−O bond energies of 3.4 eV. Terminating the surface with a monolayer of acid, as happens spontaneously in air, slightly increases these energies. In contrast, terminating the unsaturated Ti atoms with F decreases the bond energies by 65% to 1.2 eV each. Oxidation of the bridging O atoms also leads to the development of unpaired spin density on the bridging O atoms (magnetic moment = 0.17 μ_B) and somewhat less unpaired spin density on the planar surface O atoms (0.08 μ_B). Similar effects have been reported in DFT simulations of F bound to anatase TiO_2.[54]

The increased reactivity of the fluorinated surface toward etching can also be rationalized in terms of disrupted charge balance in the surface layer. The fully fluorinated surface layer has a stoichiometry of $TiO_2F_{0.5}$. Removing every other bridging O atom from the surface layer would lead to $TiO_{1.75}F_{0.5}$, a charge-balanced surface. Consistent with this simplistic rationalization, DFT simulations predict that the removal of a bridging O atom from the fully fluorinated surface to form $^1/_2$ O_2 would be exoergic by 0.47 eV.

https://doi.org/10.1021/acs.jpcc.2c00651
J. Phys. Chem. C 2022, 126, 4899−4906

DISCUSSION

Surface Morphology and Reaction Dynamics. The absence of crystallographic features in the final morphology, such as straight step edges or islands with a regular habit, suggests that the etching reactions occurred isotropically at many sites on the surface, not at a few reactive sites.[55,56] This is very different than the highly anisotropic, basic peroxide etching reaction used to create the initial flat surface, which selectively attacks step sites.[50] This is also very different than the initial fluorination reaction, which only occurred at undersaturated Ti sites.

One possible explanation for the isotropy of the etching reaction is the dynamics (not the energetics) of the XeF_2 reaction. XeF_2 is a relatively stable molecule with a total bond strength of 2.75 eV; however, the removal of one F atom produces XeF, a very unstable molecule with a bond strength of only 0.13 eV.[57] When XeF_2 reacts with a clean Si(100) surface, the first step of the reaction is the abstraction of a F atom to produce a fluorinated surface site and a scattered XeF molecule.[58,59] The XeF molecule is rovibrationally excited by a combination of the scattering process and the reaction exothermicity. As a result of this excitation, 60−90% of the scattered XeF dissociates within a few Å of the surface, producing a highly reactive F radical.[57] If the F radical is released in the direction of the surface (a statistical process), the second F atom can also react with the surface. The reaction of the second F atom is potentially 2.62 eV more exoergic than the reaction of the first atom, as there is no XeF_2 bond to break.

Because the reaction dynamics of the XeF_2/Si(100) reaction is dominated by the unusual energetics of the XeF_2 and XeF molecules, we hypothesize that similar dynamics may influence the XeF_2/TiO_2(110) reaction in two ways. First, the production of F atoms from the decomposition of XeF would introduce a much more exoergic reaction channel, as F atoms are extremely reactive. This high reactivity is consistent with an isotropic reaction and the production of a rough and bumpy surface. Second, our experiments showed that no reaction occurred when the undersaturated Ti atoms were blocked with acid adsorbed from the air. If there was no initial XeF_2 reaction, no F radicals could have been produced from the decomposition of XeF. This is consistent with our results. If F radicals were to have been produced during the reaction of XeF_2 with the acid-covered surface, the F radicals would have reacted with the adsorbed organic acids on the surface, as F reacts readily with both C−C and C−H bonds.[60] This reaction would have either created fluorinated adsorbed products or removed the acid layer entirely by producing fluorinated gaseous products. Either possibility is definitively ruled out by the photoemission spectra in Figure 2, which show that the adsorbed acid layer remained intact.

If our reasoning is correct, less reactive fluorinating agents are needed for the production of atomically smooth F-TiO_2. Two possibilities are F_2 or possibly F-TEDA (Selectfluor).[61] Because of the unusual dynamics described above, XeF_2 is a more aggressive etchant than F_2, at least on Si surfaces. XeF_2 will etch Si continuously at room temperature and is used industrially for this purpose. In contrast, F_2 does not etch Si at room temperature, as the surface becomes passivated by a thick fluorosilyl layer.[62]

Adventitious Carbon and F-TiO_2. Photoemission spectroscopists have found that almost every air-exposed surface develops a thin carbon-containing coating of uncertain origin. This film is described euphemistically as "adventitious C" and is often used to calibrate XP spectra.[63] Our study was initially motivated by the absence of adventitious C on F-containing anatase nanocrystals, which led us to hypothesize that fluorine atoms might passivate TiO_2 by binding to the undersaturated Ti atoms, forming a repellent coating.

Our initial hypothesis was correct in general, but wrong in detail. The XP spectra in Figure 2 show that F-TiO_2 does not develop an adventitious C coating, as we predicted. However, quantification of our spectra shows that only 80% of the undersaturated Ti sites are "blocked" with F. The simulation in Figure 4 explains why this partial monolayer effectively blocks the adsorption of air-borne acids and other species that require a bidentate binding site, but what about the adsorption of other carbon-containing molecules? For example, the typical partial pressure of atmospheric methanol is 10^{-2} to 10^{-3} mbar,[64] far greater than the 10^{-6}−10^{-7} mbar partial pressure typical of small organic acids.[65] We explain this difference in terms of bonding geometry. Although methanol and many other small organic molecules adsorb to TiO_2, small molecules that form monodentate bonds typically desorb near room temperature.[20,66−68] As such, even though monodentate species will transiently bond to the TiO_2 surface, they will desorb in a room temperature vacuum chamber long before the photoemission analysis is complete (or even started).

CONCLUSIONS

The photochemical degradation of a monolayer of trimethyl acetate on an atomically flat TiO_2(110) surface produced undersaturated Ti atoms that subsequently reacted with XeF_2 (g) to produce a fluorinated surface. After rinsing in H_2O, photoemission spectroscopy showed that 80% of the initially undersaturated Ti sites were covalently bound to F. This fluorine termination was surprisingly robust. Immersing the fluorinated surface in boiling H_2O for 60 min or boiling base for 10 min removed only ∼60% of the F atoms.

The fluorinated surface remained notably contamination free, even after immersion in solution and exposure to room air for tens of minutes. Photoemission spectroscopy showed that the density of adventitious C was 2.5 atoms/nm^2, which is equivalent to 0.06 ML of graphene. In contrast, the Ti sites on air-exposed clean TiO_2(110) surfaces are rapidly and completely covered with adsorbed acids. The contamination-resistant properties of the fluorinated surface were attributed to the random blocking of 80% of the undersaturated Ti atoms, which simulations showed would block 93% of bidentate binding sites. Although 20% of the monodentate binding sites presumably remain exposed, small molecules that bind to TiO_2 in a monodentate fashion typically desorb relatively quickly at room temperature.

Although the initial surface was atomically flat, the fluorinated surface was rough on an atomic scale, displaying short, atomically straight rows parallel to the [001] direction. The roughened morphology was an indication of a relatively isotropic etching reaction. This type of site non-specific etching was attributed to both the destabilization of the surface by F as well as the unusual reaction dynamics of XeF_2.

ASSOCIATED CONTENT

Supporting Information

The Supporting Information is available free of charge at https://pubs.acs.org/doi/10.1021/acs.jpcc.2c00651.

https://doi.org/10.1021/acs.jpcc.2c00651
J. Phys. Chem. C 2022, 126, 4899−4906

XPS calibration, additional XPS analysis, calibration of DFT simulations of XPS binding energies, sample structures used in DFT simulations (PDF)

AUTHOR INFORMATION

Corresponding Author

Melissa A. Hines − *Department of Chemistry and Chemical Biology, Cornell University, Ithaca, New York 14853, United States;* orcid.org/0000-0002-7960-8208; Phone: +1-607-255-3040; Email: Melissa.Hines@cornell.edu

Author

William J. I. DeBenedetti − *Department of Chemistry and Chemical Biology, Cornell University, Ithaca, New York 14853, United States*

Complete contact information is available at: https://pubs.acs.org/10.1021/acs.jpcc.2c00651

Notes

The authors declare no competing financial interest.

ACKNOWLEDGMENTS

This work was supported by the National Science Foundation under Award CHE-2107716 and used the National Energy Research Scientific Computing Center, a DOE Office of Science User Facility supported by the Office of Science of the U.S. Department of Energy (DE-AC02-05CH11231) as well as the Cornell Center for Materials Research Shared Facilities supported through the NSF MRSEC program (DMR-1719875).

REFERENCES

(1) Feldman, L. C. Introduction. *Fundamental Aspects of Silicon Oxidation*; Springer Series in Material Science; Chabal, Y. J., Ed.; Springer: 2001; pp 1−11.

(2) Jiang, Q.; Zhao, Y.; Zhang, X.; Yang, X.; Chen, Y.; Chu, Z.; Ye, Q.; Li, X.; Yin, Z.; You, J. Surface Passivation of Perovskite Film for Efficient Solar Cells. *Nat. Photonics* **2019**, *13*, 460−466.

(3) Ip, A. H.; Thon, S. M.; Hoogland, S.; Voznyy, O.; Zhitomirsky, D.; Debnath, R.; Levina, L.; Rollny, L. R.; Carey, G. H.; Fischer, A.; et al. Hybrid Passivated Colloidal Quantum Dot Solids. *Nat. Nanotechnol.* **2012**, *7*, 577−582.

(4) Higashi, G. S.; Chabal, Y. J.; Trucks, G. W.; Raghavachari, K. Ideal Hydrogen Termination of the Si(111) Surface. *Appl. Phys. Lett.* **1990**, *56*, 656−658.

(5) Hines, M. A. In Search of Perfection: Understanding the Highly Defect-Selective Chemistry of Anisotropic Etching. *Annu. Rev. Phys. Chem.* **2003**, *54*, 29−56.

(6) DeBenedetti, W. J. I.; Skibinski, E. S.; Jing, D.; Song, A.; Hines, M. A. Atomic-Scale Understanding of Catalyst Activation: Carboxylic Acid Solutions, But Not the Acid Itself, Increase the Reactivity of Anatase (001) Faceted Nanocatalysts. *J. Phys. Chem. C* **2018**, *122*, 4307−4314.

(7) Yang, H. G.; Sun, C. H.; Qiao, S. Z.; Zou, J.; Liu, G.; Smith, S. C.; Cheng, H. M.; Lu, G. Q. Anatase TiO_2 Single Crystals With a Large Percentage of Reactive Facets. *Nature* **2008**, *453*, 638−641.

(8) Balajka, J.; Hines, M. A.; DeBenedetti, W. J. I.; Komora, M.; Pavelec, J.; Schmid, M.; Diebold, U. High Affinity Adsorption Leads to Molecularly Ordered Interfaces on TiO_2 in Air and Solution. *Science* **2018**, *361*, 786−789.

(9) Barteau, M. A. Organic Reactions At Well-Defined Oxide Surfaces. *Chem. Rev.* **1996**, *96*, 1413−1430.

(10) Gordon, T. R.; Cargnello, M.; Paik, T.; Mangolini, F.; Weber, R. T.; Fornasiero, P.; Murray, C. B. Nonaqueous Synthesis of TiO_2 Nanocrystals Using TiF_4 to Engineer Morphology, Oxygen Vacancy Concentration, and Photocatalytic Activity. *J. Am. Chem. Soc.* **2012**, *134*, 6751−6761.

(11) Mrowetz, M.; Selli, E. H_2O_2 Evolution During the Photocatalytic Degradation of Organic Molecules on Fluorinated TiO_2. *New J. Chem.* **2006**, *30*, 108−114.

(12) Park, H.; Choi, W. Photocatalytic Conversion of Benzene to Phenol Using Modified TiO_2 and Polyoxometalates. *Catal. Today* **2005**, *101*, 291−297.

(13) Minero, C.; Mariella, G.; Maurino, V.; Vione, D.; Pelizzetti, E. Photocatalytic Transformation of Organic Compounds in the Presence of Inorganic Ions. 2. Competitive Reactions of Phenol and Alcohols on a Titanium Dioxide-Fluoride System. *Langmuir* **2000**, *16*, 8964−8972.

(14) Park, H.; Choi, W. Effects of TiO_2 Surface Fluorination on Photocatalytic Reactions and Photoelectrochemical Behaviors. *J. Phys. Chem. B* **2004**, *108*, 4086−4093.

(15) Mrowetz, M.; Selli, E. Enhanced Photocatalytic Formation of Hydroxyl Radicals on Fluorinated TiO_2. *Phys. Chem. Chem. Phys.* **2005**, *7*, 1100−1102.

(16) Tang, J.; Quan, H.; Ye, J. Photocatalytic Properties and Photoinduced Hydrophilicity of Surface-Fluorinated TiO_2. *Chem. Mater.* **2007**, *19*, 116−122.

(17) Zhang, P.; Tachikawa, T.; Fujitsuka, M.; Majima, T. In Situ Fluorine Doping of TiO_2 Superstructures for Efficient Visible-Light Driven Hydrogen Generation. *ChemSusChem* **2016**, *9*, 617−623.

(18) Kang, X.; Liu, S.; Dai, Z.; He, Y.; Song, X.; Tan, Z. Titanium Dioxide: From Engineering to Applications. *Catalysts* **2019**, *9*, 191.

(19) Wendt, S.; Sprunger, P. T.; Lira, E.; Madsen, G. K. H.; Li, Z.; Hansen, J. Ø.; Matthiesen, J.; Blekinge-Rasmussen, A.; Lægsgaard, E.; Hammer, B.; et al. The Role of Interstitial Sites in the Ti 3d Defect State in the Band Gap of Titania. *Science* **2008**, *320*, 1755−1759.

(20) Lira, E.; Hansen, J. Ø.; Huo, P.; Bechstein, R.; Galliker, P.; Lægsgaard, E.; Hammer, B.; Wendt, S.; Besenbacher, F. Dissociative and Molecular Oxygen Chemisorption Channels on Reduced Rutile TiO_2(110): An STM and TPD Study. *Surf. Sci.* **2010**, *604*, 1945−1960.

(21) Lira, E.; Wendt, S.; Huo, P.; Hansen, J. Ø.; Streber, R.; Porsgaard, S.; Wei, Y.; Bechstein, R.; Lægsgaard, E.; Besenbacher, F. The Importance of Bulk Ti^{3+} Defects in the Oxygen Chemistry on Titania Surfaces. *J. Am. Chem. Soc.* **2011**, *133*, 6529−6532.

(22) Skibinski, E. S.; Song, A.; DeBenedetti, W. J. I.; Ortoll-Bloch, A. G.; Hines, M. A. Solution Deposition of Self-Assembled Benzoate Monolayers on Rutile (110): Effect of π-π Interactions on Monolayer Structure. *J. Phys. Chem. C* **2016**, *120*, 11581−11589.

(23) Vaughan, J. G.; Raut, M. K. Tin Contamination During Surface Cleaning for Thermocompression Bonding. *Proc. Int. Symp. on Microelectron.* **1984**, 424−427.

(24) Kohn, W.; Sham, L. J. Self-Consistent Equations Including Exchange and Correlation Effects. *Phys. Rev.* **1965**, *140*, A1133−A1138.

(25) Zhang, Y.; Yang, W. Comment on "Generalized Gradient Approximation Made Simple. *Phys. Rev. Lett.* **1998**, *80*, 890.

(26) Kresse, G.; Hafner, J. *Ab Initio* Molecular Dynamics for Liquid Metals. *Phys. Rev. B* **1993**, *47*, 558−561.

(27) Kresse, G.; Hafner, J. *Ab Initio* Molecular-Dynamics Simulation of the Liquid-Metal-Amorphous-Semiconductor Transition in Germanium. *Phys. Rev. B* **1994**, *49*, 14251−14269.

(28) Kresse, G.; Furthmüller, J. Efficiency of *Ab-Initio* Total Energy Calculations for Metals and Semiconductors Using a Plane-Wave Basis Set. *Comput. Mater. Sci.* **1996**, *6*, 15−50.

(29) Kresse, G.; Furthmüller, J. Efficient Iterative Schemes for *Ab Initio* Total-Energy Calculations Using a Plane-Wave Basis Set. *Phys. Rev. B* **1996**, *54*, 11169−11186.

(30) Dudarev, S. L.; Botton, G. A.; Savrasov, S. Y.; Humphreys, C. J.; Sutton, A. P. Electron-Energy-Loss Spectra and the Structural Stability of Nickel Oxide: An LSDA + *U* Study. *Phys. Rev. B* **1998**, *57*, 1505−1509.

(31) Chrétien, S.; Metiu, H. Electronic Structure of Partially Reduced Rutile TiO_2(110) Surface: Where are the Unpaired Electrons Located? *J. Phys. Chem. C* **2011**, *115*, 4696−4705.
(32) Deskins, N. A.; Rousseau, R.; Dupuis, M. Distribution of Ti^{3+} Surface States in Reduced TiO_2. *J. Phys. Chem. C* **2011**, *115*, 7562−7572.
(33) Setvin, M.; Franchini, C.; Hao, X.; Schmid, M.; Janotti, A.; Kaltak, M.; Van de Walle, C. G.; Kresse, G.; Diebold, U. Direct View of Excess Electrons in TiO_2 Rutile and Anatase. *Phys. Rev. Lett.* **2014**, *113*, 086402.
(34) Grimme, S.; Antony, J.; Ehrlich, S.; Krieg, H. A Consistent and Accurate *Ab Initio* Parameterization of Density Functional Dispersion Correction (DFT-D) for the 94 Elements H-Pu. *J. Chem. Phys.* **2010**, *132*, 154104.
(35) Grimme, S.; Ehrlich, S.; Goerigk, L. Effect of the Damping Function in Dispersion Corrected Density Functional Theory. *J. Comput. Chem.* **2011**, *32*, 1456−1465.
(36) Blöchl, P. E. Projector Augmented-Wave Method. *Phys. Rev. B* **1994**, *50*, 17953−17979.
(37) Kresse, G.; Joubert, D. From Ultrasoft Pseudopotentials to the Projector Augmented-Wave Method. *Phys. Rev. B* **1999**, *59*, 1758−1775.
(38) Dozzi, M. V.; Selli, E. Doping TiO_2 With *p*-Block Elements: Effects on Photocatalytic Activity. *J. Photochem. Photobiol. C: Photochem. Rev.* **2013**, *14*, 13−28.
(39) Hansen, W. N.; Kolb, D. M. The Work Function of Emersed Electrodes. *J. Electroanal. Chem.* **1979**, *100*, 493−500.
(40) Hansen, W. N.; Kolb, D. M.; Rath, D. L.; Wille, R. An ESCA Study on Emersed Electrodes. *J. Electroanal. Chem.* **1980**, *110*, 369−373.
(41) Tang, J.; Quan, H.; Ye, J. Photocatalytic Properties and Photoinduced Hydrophilicity of Surface-Fluorinated TiO_2. *Chem. Mater.* **2007**, *19*, 116−122.
(42) Moss, J. H.; Parfitt, G. D.; Fright, A. The Fluorination of Titanium Dioxide Surfaces. *Colloid Polym. Sci.* **1978**, *256*, 1121−1130.
(43) Tius, M. A. Xenon Difluoride in Synthesis. *Tetrahedron* **1995**, *51*, 6605−6634.
(44) Henderson, M. A.; White, J. M.; Uetsuka, H.; Onishi, H. Photochemical Charge Transfer and Trapping At the Interface Between an Organic Adlayer and an Oxide Semiconductor. *J. Am. Chem. Soc.* **2003**, *125*, 14974−14975.
(45) Uetsuka, H.; Onishi, H.; Henderson, M. A.; White, J. M. Photoinduced Redox Reaction Coupled With Limited Electron Mobility At Metal Oxide Surface. *J. Phys. Chem. B* **2004**, *108*, 10621−10624.
(46) White, J. M.; Henderson, M. A. Trimethyl Acetate on TiO_2(110): Preparation and Anaerobic Photolysis. *J. Phys. Chem. B* **2005**, *109*, 12417−12430.
(47) Henderson, M. A. A Surface Science Perspective on TiO_2 Photocatalysis. *Surf. Sci. Reports* **2011**, *66*, 185−297.
(48) DeBenedetti, W. J. I.; Hines, M. A. Breaking π-π Interactions in Carboxylic Acid Monolayers on Rutile TiO_2(110) Leads to Unexpected Long-Range Ordering. *J. Phys. Chem. C* **2019**, *123*, 8836−8842.
(49) Davis, D. W.; Banna, M. S.; Shirley, D. A. Core-Level Binding-Energy Shifts in Small Molecules. *J. Chem. Phys.* **1974**, *60*, 237−245.
(50) Song, A.; Skibinski, E. S.; DeBenedetti, W. J. I.; Ortoll-Bloch, A. G.; Hines, M. A. Nanoscale Solvation Leads to Spontaneous Formation of a Bicarbonate Monolayer on Rutile (110) Under Ambient Conditions: Implications for CO_2 Photoreduction. *J. Phys. Chem. C* **2016**, *120*, 9326−9333.
(51) Song, A.; Jing, D.; Hines, M. A. Rutile Surface Reactivity Provides Insight Into the Structure-Directing Role of Peroxide in TiO_2 Polymorph Control. *J. Phys. Chem. C* **2014**, *118*, 27343−27352.
(52) Diebold, U. The Surface Science of Titanium Dioxide. *Surf. Sci. Reports* **2003**, *48*, 53−229.
(53) LaFemina, J. P. Total Energy Computations of Oxide Surface Reconstructions. *Crit. Rev. Surf. Chem.* **1994**, *3*, 297−386.
(54) Lamiel-Garcia, O.; Tosoni, S.; Illas, F. Relative Stability of F-Covered TiO_2 Anatase (101) and (001) Surfaces From Periodic DFT Calculations and *Ab Initio* Atomistic Thermodynamics. *J. Phys. Chem. C* **2014**, *118*, 13667−13673.
(55) Hines, M. A. The Picture Tells the Story: Using Surface Morphology to Probe Chemical Etching Reactions. *Int. Reviews in Phys. Chem.* **2001**, *20*, 645−672.
(56) Hines, M. A. In Search of Perfection: Understanding the Highly Defect-Selective Chemistry of Anisotropic Etching. *Annu. Rev. Phys. Chem.* **2003**, *54*, 29−56.
(57) Tellinghuisen, P. C.; Tellinghuisen, J.; Coxon, J. A.; Velazco, J. E.; Setser, D. W. Spectroscopic Studies of Diatomic Noble Gas Halides. IV. Vibrational and Rotational Constants for the *X*, *B*, and *D* States of XeF. *J. Chem. Phys.* **1978**, *68*, 5187−5198.
(58) Hefty, R. C.; Holt, J. R.; Tate, M. R.; Ceyer, S. T. Atom Abstraction and Gas Phase Dissociation in the Interaction of XeF_2 With Si(100). *J. Chem. Phys.* **2008**, *129*, 214701.
(59) Hefty, R. C.; Holt, J. R.; Tate, M. R.; Ceyer, S. T. Mechanism and Dynamics of the Reaction of Xef_2 With Fluorinated Si(100): Possible Role of Gas Phase Dissociation of a Surface Reaction Product in Plasmaless Etching. *J. Chem. Phys.* **2009**, *130*, 164714.
(60) Parson, J. M.; Shobatake, K.; Lee, Y. T.; Rice, S. A. Substitution Reactions of Fluorine Atoms With Unsaturated Hydrocarbons. *Faraday Discuss. Chem. Soc.* **1973**, *55*, 344−356.
(61) Tarantino, G.; Hammond, C. Catalytic Formation of C(sp^3)-F Bonds Via Heterogeneous Photocatalysis. *ACS Catal.* **2018**, *8*, 10321−10330.
(62) McFeely, F. R.; Morar, J. F.; Himpsel, F. J. Soft X-Ray Photoemission Study of the Silicon-Fluorine Etching Reaction. *Surf. Sci.* **1986**, *165*, 277−287.
(63) Greczynski, G.; Hultman, L. C 1*s* Peak of Adventitious Carbon Aligns to the Vacuum Level: Dire Consequences for Material's Bonding Assignment By Photoelectron Spectroscopy. *ChemPhysChem* **2017**, *18*, 1507−1512.
(64) Heikes, B. G.; Chang, W.; Pilson, M. E. Q.; Swift, E.; Singh, H. B.; Guenther, A.; Jacob, D. J.; Field, B. D.; Fall, R.; Riemer, D.; Brand, L. Atmospheric Methanol Budget and Ocean Implication. *Global Biogeochem. Cycles* **2002**, *16*, 1133.
(65) Khare, P.; Kumar, N.; Kumari, K. M.; Srivastava, S. S. Atmospheric Formic and Acetic Acids: An Overview. *Rev. Geophys.* **1999**, *37*, 227−248.
(66) Suzuki, S.; Yamaguchi, Y.; Onishi, H.; Sasaki, T.; Fukui, K.-I.; Iwasawa, Y. Studies of Pyridine and Its Derivative Adsorbed on a TiO_2(110)−(1 × 1) Surface By Means of STM, TDS, XPS, and MD Calculation in Relation to Surface Acid-Base Interaction. *J. Chem. Soc., Faraday Trans.* **1998**, *94*, 161−166.
(67) Li, Z.; Smith, R. S.; Kay, B. D.; Dohnalek, Z. Determination of Absolute Coverages for Small Aliphatic Alcohols on TiO_2(110). *J. Phys. Chem. C* **2011**, *115*, 22534−22539.
(68) Petrik, N. G.; Henderson, M. A.; Kimmel, G. A. Insights Into Acetone Photochemistry on Rutile TiO_2(110). 2. New Photodesorption Channel With CH_3 Ejection Along the Surface Normal. *J. Phys. Chem. C* **2015**, *119*, 12273−12282.

https://doi.org/10.1021/acs.jpcc.2c00651
J. Phys. Chem. C 2022, 126, 4899−4906